J Mater Sci (2007) 42:6133–6138
DOI 10.1007/s10853-006-1070-z

Comparative study of magnesium ferrite nanocrystallites prepared by sol–gel and coprecipitation methods

Cui-Ping Liu · Ming-Wei Li · Zhong Cui · Juan-Ru Huang · Yi-Ling Tian · Tong Lin · Wen-Bo Mi

Received: 7 April 2006 / Accepted: 26 September 2006 / Published online: 16 April 2007

Abstract Magnesium ferrite particles consisting of nanocrystallites were synthesized by sol–gel and coprecipitation methods. Their mean crystalline size increased with increasing calcination temperature. At the same calcination temperature, the sol–gel-derived sample always had bigger mean crystalline size than the coprecipitation-derived sample, implying that the sol–gel method facilitated the formation of magnesium ferrite crystallites. Most of the sol–gel-derived magnesium ferrite particles had a lamellar structure consisting of nanocrystallites, which were probably derived from the porous dried gel precursor. The magnesium ferrite particles had superparamagnetic properties at 27 °C, and their saturation magnetization increased with increasing size.

C.-P. Liu · M.-W. Li (✉) · Z. Cui · J.-R. Huang · Y.-L. Tian · T. Lin
Department of Chemistry, Tianjin University, Tianjin 300072, P.R. China
e-mail: mingweili@eyou.com

C.-P. Liu
Department of Material Engineering, Tianjin Institute of Urban Construction, Tianjin 300084, P.R. China

W.-B. Mi
Tianjin Key Laboratory of Low Dimensional Materials Physics and Preparing Technology, Institute of Advanced Materials Physics, Faculty of Science, Tianjin University, Tianjin 300072, P.R. China

Introduction

Spinel-type magnesium ferrite ($MgFe_2O_4$) is composed of binary oxides and has both special crystal and electron structures. When its crystallite size is below a certain value, $MgFe_2O_4$ possesses unique superparamagnetic properties at room temperature and has promising potential for applications in transformers, ferrofluids, and magnet cores of coils [1–4]. In addition, $MgFe_2O_4$ has lots of other applications, including semiconductors [5, 6], catalysts [7–10], gas sensors [11, 12] and brown pigments [13, 14].

It has been reported that high-energy milling could reduce the crystallite size of $MgFe_2O_4$ to nanometer range, but this physical process not only needed higher energy consumption but also easily induced structural disorder in the crystallites [15–17]. At present, several chemical methods, including coprecipitation [1, 3, 6, 9, 10, 13], solid-state reactions [5, 11, 12], supercritical drying processes [2, 8], micelle routes [4] and hydrothermal synthesis [18, 19], have been used to prepare $MgFe_2O_4$ nanoparticles. Both solid-state reactions and coprecipitation are economical for producing large quantities of nanoparticles, but undesired non-uniform particles were easily formed due to the agglomeration of nanoparticles.

Alternatively, sol–gel is another efficient method for preparing nanomaterials at moderate conditions, and it is believed that sol–gel-derived nanoparticles generally possessed good chemical homogeneity, high purity and lower calcination temperature [14, 20].

In the present work, $MgFe_2O_4$ nanocrystallites were prepared by sol–gel and coprecipitation methods. The structures and magnetic properties of the samples were analyzed and compared. The samples prepared by different methods had obvious differences in morphology. It was found that the sol–gel method facilitated the formation of

lamellar $MgFe_2O_4$ particles, which consisted of many nanocrystallites and possessed superparamagnetic properties.

Experimental

In the sol–gel method, a definite stoichiometric molar proportion (0.016 mol/0.008 mol) of $Fe(NO_3)_3{\cdot}9H_2O$ and $Mg(NO_3)_2{\cdot}6H_2O$ were dissolved in 20 mL deionized water to form an aqueous mixture. Then 0.036 mol citric acid powders were dissolved in the mixture. When the mixture was being magnetically stirred at 60 °C, about 12 mL ammonia water (25%) was dripped into the mixture to adjust its pH to 7.0, and the mixture was transformed into sol. After stirred for about 10 h, the sol was turned into black gel. The gel was dried at 120 °C for 12 h with its volume expanding about 10 times. Finally, the dried gel was ground and calcined for 2 h until the brown product formed. To study the effect of calcination temperature on the product, the calcination temperature was varied from 400 to 800 °C.

In the coprecipitation method, the same above-mentioned aqueous mixture of definite stoichiometric proportion of $Fe(NO_3)_3{\cdot}9H_2O$ and $Mg(NO_3)_2{\cdot}6H_2O$ was prepared first. Then some 0.1 M sodium hydroxide solution was dripped into the mixture to keep its pH between 9.0 and 10.0. As a result, there was black precipitate appeared. The precipitate was filtrated and washed with deionized water until its pH became neutral. Finally, the precipitate was dried at 120 °C for 4 h and then was calcined at different temperature ranging from 400 to 800 °C for 2 h until the brown product formed.

To study the thermal stability of both the two precursors dried gel and dried precipitate, thermogravimetric and differential thermal analyses (TG–DTA) were performed using a ZRY-2P simultaneous thermal analyzer. About 10 mg sample was heated from room temperature to 800 °C in air at a heating rate of 15 °C/min.

The crystalline structures of the samples were analyzed by an X'Pert Pro powder X-ray diffractometer (XRD) using Co K_α radiation. The mean crystalline size was calculated using Scherrer formula, $d = K\lambda/(\beta{\cdot}\cos\theta)$, where d (nm) is the mean crystallite size, K (=0.89) is the shape factor, λ (=0.178901 nm) is the X-ray wavelength, β (radian) is the half-width of the main diffraction peak, and θ (radian) is the Bragg angle of main diffraction peak. Morphology and microstructure of the samples were investigated using a Philips XL30ESEM scanning electron microscope (SEM) and a Tecnai G^2 F20 field-emission high-resolution transmission electron microscope (HRTEM). Magnetic properties of the samples were measured using an LDJ 9600-1 vibrating sample magnetometer (VSM) at 27 °C under a magnetic field of 10 kOe.

Results and discussion

TG–DTA curves of the dried precipitate are shown in Fig. 1a. When the temperature was increased from room temperature to 800 °C, the dried precipitate lost about 31% of its weight as shown in the TG curve. About 31% is close to the percentage of water (35%) produced in the reaction of $Mg(OH)_2 + 2Fe(OH)_3 \rightarrow MgFe_2O_4 + 4H_2O$, implying that the weight loss possible resulted from the reaction. The DTA curve shows a broad exothermic peak centered at 190 °C, which was probably caused by the formation of Fe_2O_3 from $Fe(OH)_3$ [21]. Both the TG and DTA curves are rough below 680 °C, indicated that the crystallites were formed in a wide temperature range. However, as shown in Fig. 1b, the dried gel had a weight loss of about 87% in the same temperature range. The DTA curve exhibits a sharp exothermic peak at 224 °C, and the TG curve shows that most of the weight loss also occurred around this temperature. It probably resulted from the oxidation of organic matter. It is noticeable that the TG curve becomes smooth and the DTA curve rises linearly with increasing temperature over 470 °C, implying that almost all the crystallites were formed below 470 °C. Comparing with the coprecipitation method, the sol–gel method facilitated the formation of $MgFe_2O_4$ crystallites at lower temperature.

Two typical XRD spectra of the samples are shown in Fig. 2. Curve (a) is for the coprecipitation-derived sample, and curve (b) is for the sol–gel-derived sample. The spinel structure of $MgFe_2O_4$, which was described in JCPDS 88-1942, was detected in both samples. Seven peaks center at 2θ = 21.238°, 35.075°, 41.442°, 50.466°, 67.361°, 74.229°, and 88.818°, which coincide with $MgFe_2O_4$ crystal faces (1 1 1) (d_1 = 0.4854 nm), (2 2 0) (d_2 = 0. 2969 nm), (3 1 1) (d_3 = 0.2528 nm), (4 0 0) (d_4 = 0.2098 nm), (5 1 1) (d_5 = 0.1613 nm), (4 4 0) (d_6 = 0.1482 nm), and (5 3 3) (d_7 = 0.1278 nm), respectively. Additionally, little Fe_2O_3 was detected in both the two samples, and similar cases have been reported previously [1, 14].

As shown in Fig. 3, the samples' mean crystalline size calculated using Scherrer formula was in nanometer range, and it increased with increasing calcination temperature. At the same calcination temperature, the sol–gel-derived sample always had bigger mean crystalline size than the coprecipitation-derived sample, indicating that the sol–gel method facilitated the formation of $MgFe_2O_4$ crystallites. This result could also be approved by the higher and narrower peaks appearing in the XRD spectrum of the sol–gel-derived sample.

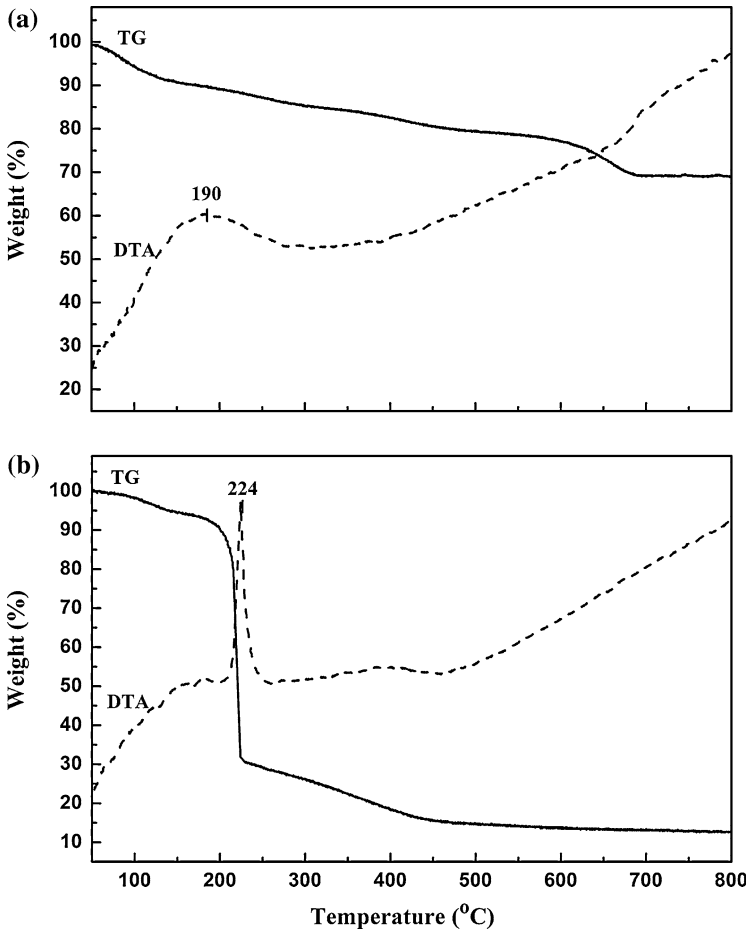

Fig. 1 TG–DTA curves of the precursors used in producing $MgFe_2O_4$ nanocrystallites: (**a**) dried precipitate, and (**b**) dried gel powders

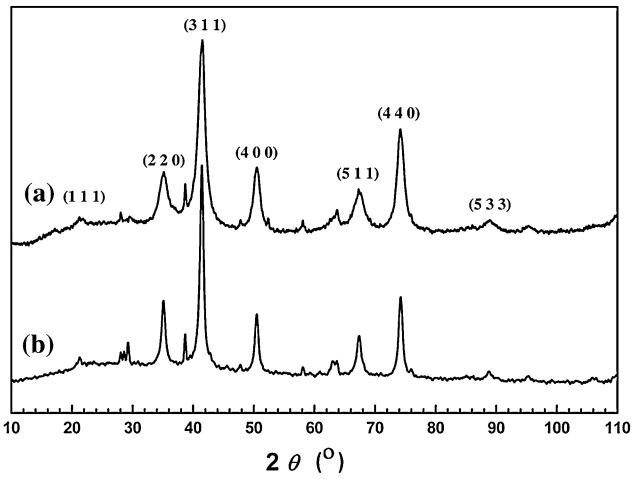

Fig. 2 XRD spectra of the $MgFe_2O_4$ nanocrystallites: (**a**) coprecipitation-derived sample, and (**b**) sol–gel-derived sample. Calcination temperature: 600 °C

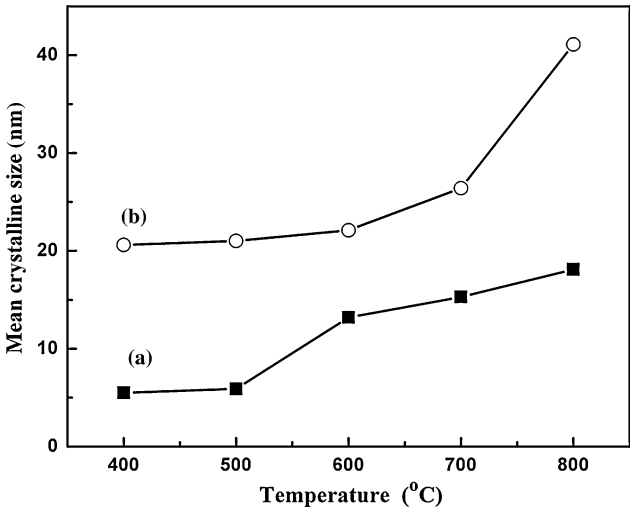

Fig. 3 Variation of the mean crystalline size of $MgFe_2O_4$ nanocrystallites with the calcination temperature: (**a**) coprecipitation-derived sample, and (**b**) sol–gel-derived sample

There were obvious differences between the samples' morphologies, as depicted in the SEM images with the same magnification (see Fig. 4). The coprecipitation-derived sample consisted of many granules. The size of most particles was in micron range, implying that the granules were the congeries of nanocrystallites. However, there were

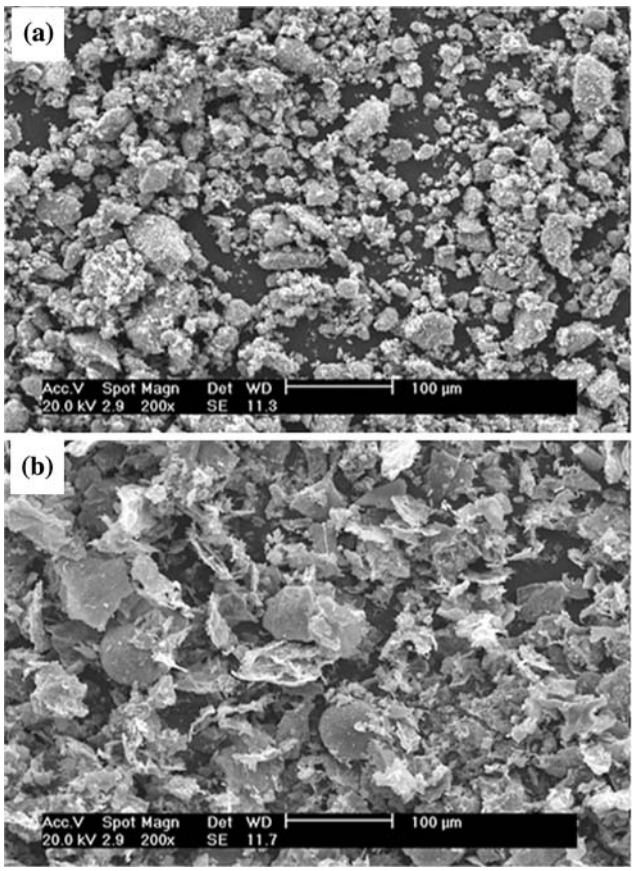

Fig. 4 SEM images of $MgFe_2O_4$ nanocrystallites: (**a**) coprecipitation-derived sample, and (**b**) sol–gel-derived sample. Calcination temperature: 600 °C

many lamellar particles in the sol–gel-derived sample. The particles were very thin, and their plane size was generally in micron range. We speculate that the lamellar particles were assembled by nanocrystallites arranged along the planes. The samples' morphologies were relative to the preparing processes and should influence their magnetic properties.

To clarify the microstructures of the samples, their HRTEM images are shown in Figs. 5, 6. At low magnification, most of the coprecipitation-derived particles were in an agglomeration state (see Fig. 5a). Figure 5b probably shows a piece of the lamellar sol–gel-derived particle due to its size being similar to the particle's shown in Fig. 4b. The particle consisted of many tiny particles with relatively uniform size. The insets of Fig. 5 are the selected-area electron diffraction patterns of the samples, and they indicate that the sol–gel-derived sample was better crystallized than the coprecipitation-derived one.

The high-magnification Fig. 6a exhibits that the coprecipitation-derived particles had some different lattice spaces. For example, there were lattice space of 0.49, 0.30 and 0.25 nm, corresponding to the (1 1 1), (2 2 0) and (3 1 1) atomic planes of $MgFe_2O_4$, respectively. However, the sol–gel-derived sample possessed bigger mean crystalline size, and its (2 2 0) atomic planes appeared more often. The samples show many aforementioned $MgFe_2O_4$ crystal faces calculated by Scherrer formula, implying that they mainly consisted of single-crystalline nanoparticles.

Superparamagnetic behavior at room temperature is a unique property of $MgFe_2O_4$ nanomaterials. Figure 7 shows the magnetic hysteresis loops of the samples. The remanent magnetization of the samples was close to zero, indicating that the samples were superparamagnetic. With increasing calcination temperature and increasing crystalline size, the saturation magnetization of coprecipitation-derived samples increased from 2.2 to 5.8 emu/g, and the saturation magnetization of sol–gel-derived ones increased

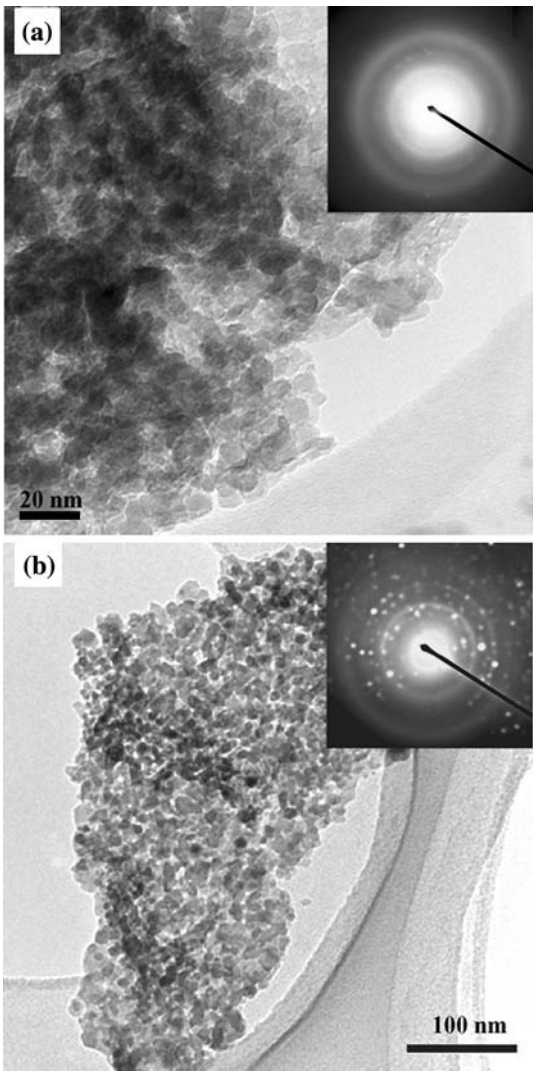

Fig. 5 HRTEM images of $MgFe_2O_4$ nanocrystallites at low magnification: (**a**) coprecipitation-derived sample, and (**b**) sol–gel-derived sample. The insets are their corresponding diffraction pattern. Calcination temperature: 600 °C

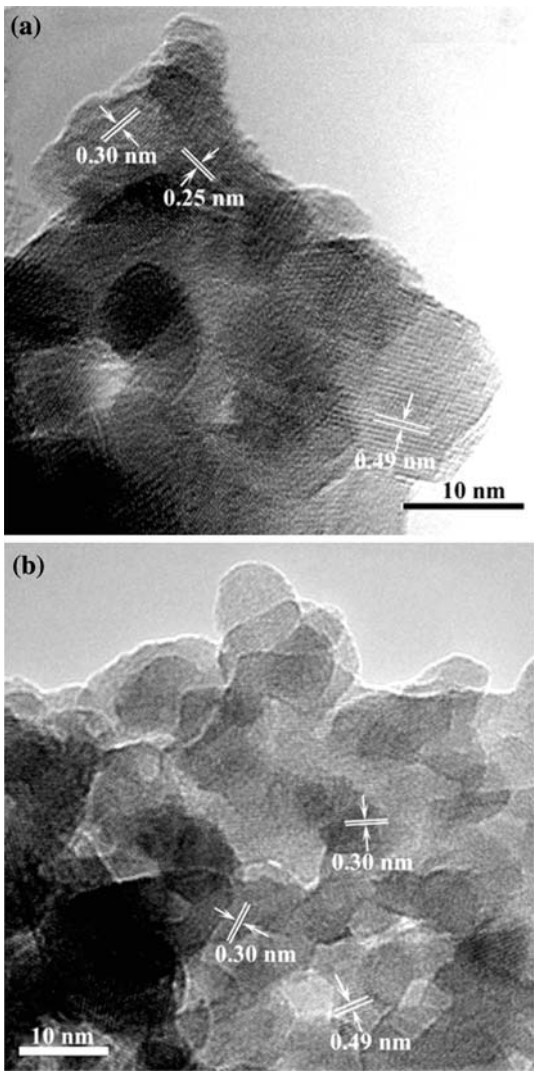

Fig. 6 HRTEM images of $MgFe_2O_4$ nanocrystallites at high magnification: (**a**) coprecipitation-derived sample, and (**b**) sol–gel-derived sample. Calcination temperature: 600 °C

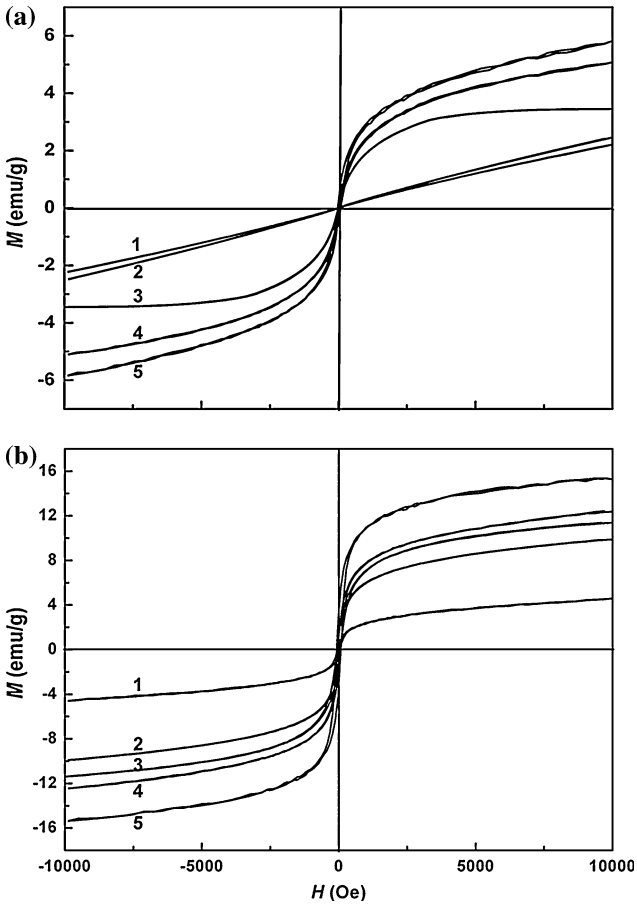

Fig. 7 Magnetic hysteresis loops measured at 27 °C for $MgFe_2O_4$ nanocrystallites: (**a**) coprecipitation-derived sample, and (**b**) sol–gel-derived sample. Calcination temperature: (1) 400, (2) 500, (3) 600, (4) 700, and (5) 800 °C

from 4.6 to 15.3 emu/g. The correlation between the saturation magnetization of $MgFe_2O_4$ nanocrystallites and their size is consistent with the literature [1]. The coprecipitation-derived samples prepared at calcination temperature of 400 and 500 °C had obviously low saturation magnetization (curves 1 and 2 in Fig. 7a). It probably resulted from the smaller crystallites whose mean crystalline size was below 6 nm shown in Fig. 3. In addition, the samples' saturation magnetization was lower than the bulk $MgFe_2O_4$ material (approximately 30 emu/g [22]), reflecting their nanocrystalline character.

As mentioned early, the sol–gel-derived particles possessed a lamellar structure. We suggested that this unique structure was formed in the sol–gel process. When the sol was turned into gel, there was a three-dimensional framework formed, which contained much water. When the gel was dried at 120 °C, its volume expanded about 10 times due to water evaporation, hence many pores were formed within the dried gel. The porous dried gel was ground and calcined to prepare nanocrystallites. We speculate that the pore walls shaped the lamellar structure of the final $MgFe_2O_4$ particles. The majority of dried gel was oxidized and escaped when it was calcined at around 224 °C. As a result, the lamellar sol–gel-derived particles consisted of lots of tiny nanocrystallites, which were more easily formed at lower calcination temperature.

Conclusions

In summary, magnesium ferrite nanocrystallites were successfully prepared by sol–gel and coprecipitation methods. The samples' mean crystalline size increased with increasing calcination temperature. The sol–gel-derived samples consisted of lots of lamellar particles, which were probably derived from the porous dry gel formed during the sol–gel process. Comparing to the granular coprecipi-

tation-derived particles, the lamellar sol–gel-derived $MgFe_2O_4$ particles possessed bigger mean crystalline size and higher saturation magnetization. This investigation indicates that the sol–gel method is efficient for synthesizing $MgFe_2O_4$ particles possessing unique microstructures and superparamagnetic properties.

Acknowledgements This research was partially financial supported by the Natural Science Foundation of China (project No. 20476071).

References

1. Chen Q, Zhang ZJ (1998) Appl Phys Lett 73:3156
2. Oliver SA, Willey RJ, Hamdeh HH, Oliveri G, Busca G (1995) Scripta Metall Mater 33:1695
3. Chen Q, Rondinone AJ, Chakoumakos BC, Zhang ZJ (1999) J Magn Magn Mater 194:1
4. Liu C, Zou B, Rondinone AJ, Zhang ZJ (2000) J Am Chem Soc 122:6263
5. Reddy PV, Satyanarayana R, Rao TS (1984) J Mater Sci Lett 3:847
6. Benko FA, Koffyberg EP (1986) Mater Res Bull 21:1183
7. Yang BL, Cheng DS, Lee SB (1991) Appl Catal 70:161
8. Willey RJ, Noirclerc P, Busca G (1993) Chem Eng Commun 123:1
9. Xiong C, Chen Q, Lu W, Gao H, Lu W, Gao Z (2000) Catal Lett 69:231
10. Lee YH, Lee GD, Park SS, Hong SS (2005) React Kinet Catal Lett 84:311
11. Gusmano G, Montesperelli G, Nunziante P, Traversa E (1993) J Mater Sci 28:6195
12. Liu Y-L, Liu Z-M, Yang Y, Yang H-F, Shen G-L, Yu R-Q (2005) Sens Actuators B 107:600
13. Hana SB, Abdel-Mohsen FF, Emira HS (2005) Int Ceram Rev 54:106
14. Abdel-Mohsen FF, Emira HS (2005) Pigment Resin Technol 34:312
15. Šepelák V, Baabe D, Litterst FJ, Becker KD (2000) J Appl Phys 88:5884
16. Šepelák V, Menzel M, Becker KD, Krumeich F (2002) J Phys Chem B 106:6672
17. Pradhan SK, Bid S, Gateshki M, Petkov V (2005) Mater Chem Phys 93:224
18. Verma S, Potdar HS, Date SK, Joy PA (2004) In: Glembocki OJ, Hunt CE (eds) Nanoparticles and nanowire building blocks-synthesis, processing, characterization and theory. Materials Research Society, PA, USA, p 83
19. Huang YJ, Wang J, Chen QW (2005) Chin J Inorg Chem 21:697
20. Cui H, Zayat M, Levy D (2005) J Sol–Gel Sci Technol 35:175
21. Yen FS, Chen WC, Yang JM, Hong CT (2002) Nano Lett 2:245
22. Krupička S, Novák P (1982) In: Wohlfarth EP (ed) Ferromagnetic materials, vol 3. North-Holland Publishing Company, Amsterdam, p 291